journal

J. Am. Ceram. Soc., 92 [10] 2242–2246 (2009)
DOI: 10.1111/j.1551-2916.2009.03185.x

Bi_2O_3–MoO_3 Binary System: An Alternative Ultralow Sintering Temperature Microwave Dielectric

Di Zhou,[†,‡,§] Hong Wang,[‡] Li-Xia Pang,[‡] Clive A. Randall,[§] and Xi Yao[‡]

[‡]Electronic Materials Research Laboratory, Key Laboratory of the Ministry of Education, Xi'an Jiaotong University, Xi'an 710049, China

[§]Center for Dielectric Studies, Materials Research Institute, The Pennsylvania State University, University Park, Pennsylvania 16802

Preparation, phase composition, microwave dielectric properties, and chemical compatibility with silver and aluminum electrodes were investigated on a series of single-phase compounds in the Bi_2O_3–MoO_3 binary system. All materials have ultralow sintering temperatures $<820^\circ$C. Eight different xBi_2O_3–$(1-x)MoO_3$ compounds between $0.2 \le x \le 0.875$ were fabricated and the associated microwave dielectric properties were studied. The β-$Bi_2Mo_2O_9$ single phase has a positive temperature coefficient of resonant frequency (TCF) about +31 ppm/°C, with a permittivity $\varepsilon_r = 38$ and $Q_f = 12\,500$ GHz at 300 K and at a frequency of 6.3 GHz. The α-$Bi_2Mo_3O_{12}$ and γ-Bi_2MoO_6 compounds both have negative temperature coefficient values of TCF ~ -215 and ~ -114 ppm/°C, with permittivities of $\varepsilon_r = 19$ and 31, $Q_f = 21\,800$ and 16 700 GHz at 300 K measured at resonant frequencies of 7.6 and 6.4 GHz, respectively. Through sintering the Bi_2O_3–$2.2MoO_3$ at 620°C for 2 h, a composite dielectric containing both α and β phase can be obtained with a near-zero temperature coefficient of frequency TCF = −13 ppm/°C and a relative dielectric constant $\varepsilon_r = 35$, and a large $Q_f \sim 12\,000$ GHz is also observed. Owing to the frequent difficulty of thermochemical interactions between low sintering temperature materials and the electrode materials during the cofiring, preliminary investigations are made to determine any major interactions with possible candidate electrode metals, Ag and Al. From the above results, the low sintering temperature, good microwave dielectric properties, chemical compatibility with Al metal electrode, nontoxicity and price advantage of the Bi_2O_3–MoO_3 binary system, all indicate the potential for a new material system with ultralow temperature cofiring for multilayer devices application.

I. Introduction

With the rapid development of mobile communication and satellite communication, microwave electronic devices are required to be developed and fabricated for miniaturization and integration. The low-temperature-cofired ceramic technology (LTCC) becomes an important fabricating technology that can integrate the passive components within a monolithic bulk module with IC chips mounted on its surface. By this technology, microwave dielectrics are stacked in multilayers and cofired with internal electrodes, such as Ag, Cu, Au, Al, their alloys etc., in special patterns to fulfill different electrical functions.[1,2]

There are a number of excellent microwave materials with sintering temperatures ≥ 1000°C. These include materials in the following systems: ZnO–Nb_2O_5,[3,4] $Bi(Nb,Ta,Sb)O_4$,[5–7] BaO–TiO_2–Nb_2O_5 system,[8,9] Li_2O–Nb_2O_5–TiO_2,[10,11] (Zr,Sn)TiO_4,[12,13] and the most popular $(A_1A_2)(B_1B_2)O_3$ complex perovskite system.[14–16] There has been a number of attempts to use sintering aids to lower the sintering temperatures of these systems, which have had limited success. Typical sintering aids, such as V_2O_5, CuO, Bi_2O_3, and B_2O_3, lower the sintering temperatures but also increase the dielectric loss ($\sim 1/Q$). Hence, a more fruitful approach has been made to investigate new compounds with intrinsically lower sintering temperatures; some of these important binary systems include Bi_2O_3–TeO_2, TiO_2–TeO_2, CaO–TeO_2, BaO–TeO_2, ZnO–TeO_2 binary systems, BaO–TiO_2–TeO_2 ternary system, and $Bi_2W_2O_9$ systems.[17–24]

In a recent investigation, we demonstrated that a single-phase $Bi_2Mo_2O_9$ could be sintered at temperature ~ 620°C and that this material also possessed excellent dielectric properties at frequencies in the microwave range. $Bi_2Mo_2O_9$ have been shown to have a relative dielectric permittivity ~ 38, $Q_f \sim 12\,500$ GHz and a temperature coefficient of resonant frequency (TCF) around +31 ppm/°C.[25] Based on this finding and the reported low melting temperatures of many compounds in Bi_2O_3–MoO_3 binary system, a more expansive investigation was made to access the microwave properties of these compounds. In this work, we will report on the sintering temperatures and the microwave dielectric properties of nearly all the intermediate compounds in Bi_2O_3–MoO_3 binary system. There is also a preliminary assessment of the thermochemical compatibility between these compounds and electrode materials Ag and Al at the cofiring temperatures.

II. Experimental Procedure

Proportionate amounts of reagent-grade starting materials of Bi_2O_3 (>99%, Shu-Du Powders Co. Ltd., Chengdu, China) and MoO_3 (>99%, Fuchen Chemical Reagents, Tianjin, China) were prepared by mixed-oxide approach according to the following stoichiometries: Bi_2O_3–$4MoO_3$, $Bi_2Mo_3O_{12}$, Bi_2O_3–$2.2MoO_3$, $Bi_2Mo_2O_9$, $1.3Bi_2O_3$–MoO_3, $3Bi_2O_3$–$2MoO_3$, and $7Bi_2O_3$–MoO_3 compositions. Powders were mixed and milled for 4 h using a planetary mill (Nanjing Machine Factory, Nanjing, China) operating at a running speed of 150 rpm with the Zirconia balls (2 mm in diameter) used as milling media. The mixed oxides were calcined at temperatures between 600° and 750°C for 4 h for each of the different compositions (the calcination temperatures are a little lower than the densification temperatures of ceramic according to the following results). After being crushed, the powders were remilled for 5 h using ZrO_2 balls and deionized water solvent. Then dried powders were mixed with PVA binder and granulated, and then these powders were pressed into cylinders (10 mm in diameter and 5 mm in

X. M. Chen—contributing editor

Manuscript No. 25819. Received January 30, 2009; approved April 28, 2009.
This work was supported by the National 973-project of China (2009CB623302), National 863-project of China (2006AA03Z0429), and NSFC projects of China (60871044, 50835007).
[†]Author to whom correspondence should be addressed. e-mail: zhoudi1220@gmail.com

height) in a steel die under a uniaxial pressure of 200 MPa. After debinding the samples were sintered at various temperatures ranging from 600° to 850°C for 2 h. To investigate the chemical compatibility of Bi_2O_3–MoO_3 compounds with Ag and Al powders, 20 wt% Ag and 20 wt% Al were mixed with the different compounds and held at the sintering temperatures for 4 h.

The crystalline structures were investigated using X-ray diffraction (XRD) with Cu$K\alpha$ radiation (Rigaku D/MAX-2400 X-ray diffractometer, Tokyo, Japan). Microstructures of cofired ceramics were observed on the fracture surface with scanning electron microscopy (JSM-6460, JEOL, Tokyo, Japan). The dielectric properties were measured at microwave frequency by the $TE_{01\delta}$ shielded cavity method with a network analyzer (8720ES, Agilent, Palo Alto, CA) and a temperature chamber (Delta 9023, Delta Design, Poway, CA). The TCF, τ_f, was calculated using the following formula:

$$\tau_f = \frac{f_{85} - f_{25}}{f_{25} \times (85 - 25)} \quad (1)$$

where f_{85} and f_{25} were the $TE_{01\delta}$ resonant frequencies at 85° and 25°C, respectively.

III. Results and Discussion

The phase diagram and intermediate compounds of the Bi_2O_3–MoO_3 system have been studied by many researchers over the past four decades and it is now fairly well understood for Bi/Mo≤2.6.[26–36] A redrawn phase diagram and the densification temperatures found in this study are shown in Fig. 1(a), at this point (solid solution regions are ignored). Belyaev and Smolyaninov[34] and Bleijenberg *et al.*[35] reported two congruently melting compounds, Bi_2O_3–$3MoO_3$ (α) and Bi_2O_3–MoO_3 (γ), in the region 0–50 mol% Bi_2O_3. Erman *et al.*[27,28,36] found additional compounds, Bi_2O_3–$2MoO_3$ (β) and (ε) phases having solid solubility with a composition of xBi_2O_3–MoO_3 ($1.3 < x < 1.4$). Phases $7Bi_2O_3$–MoO_3 (μ) and $3Bi_2O_3$–MoO_3 are low- and high-temperature forms of $3Bi_2O_3$–$2MoO_3$ and were also identified by XRD as reported by Egashira *et al.*[27] in Bi_2O_3-rich region. The MoO_3-rich region of the Bi_2O_3–MoO_3 binary system showed very low reaction temperatures and melting temperatures below 700°C. In Bi_2O_3-rich region the melting temperatures are always below 1000°C as shown in Fig. 1(a).

The X-ray diffraction patterns for different compositions of Bi_2O_3–MoO_3 compounds sintered at their respective densification temperatures are shown in Fig. 2. Pure-phase dense bulk ceramics for α-$Bi_2Mo_3O_{12}$, β-$Bi_2Mo_2O_9$, γ-Bi_2MoO_6, ε-$Bi_{26}Mo_{10}O_{69}$, and μ-$7Bi_2O_3$–MoO_3 were all obtained, with relative densities above 96% with the exception of α-$Bi_2Mo_3O_{12}$ having a value at about 93%. For the Bi_2O_3–$4MoO_3$ sample, MoO_3 and α-$Bi_2Mo_3O_{12}$ phases were found. The Bi_2O_3–$2.2MoO_3$ composition consisted of both α and β phases. All the compounds have low sintering temperatures below 850°C as shown in Fig. 1(a). The typical crystal structures and coordination numbers of both Mo and Bi are shown in Fig. 1(b). The α-$Bi_2Mo_3O_{12}$, β-$Bi_2Mo_2O_9$, γ-Bi_2MoO_6, and ε-$Bi_{26}Mo_{10}O_{69}$ phases have low crystal symmetries with a monoclinic structure. The space groups of α-$Bi_2Mo_3O_{12}$ and β-$Bi_2Mo_2O_9$ are both $P2_1/n$ (14). The space groups of γ-Bi_2MoO_6 and ε-$Bi_{26}Mo_{10}O_{69}$ are $P2_1/c$ (14) and $P2/a$ (13), respectively. The μ-$7Bi_2O_3$–MoO_3 compound has a tetragonal symmetry within this phase ($I4/m$, number 87). The coordination environment and bonding of the molybdenum cation have been investigated previously in various molybdate phases. The molybdenum coordination is mostly found to be fivefold[37] for the α-$Bi_2Mo_3O_{12}$, where there are also distortions in the form of four short Mo–O bonds and intermediate bond length for each of the three Mo sites. In the Buttrey *et al.*'s[33] study, there is evidence of a tetrahedral Mo coordination in both the β-$Bi_2Mo_2O_9$ and γ-Bi_2MoO_6 and the tetrahedra are also somewhat distorted. The molybdenum coordination of ε-$Bi_{26}Mo_{10}O_{69}$ is basically tetrahedral, but more distorted than that of

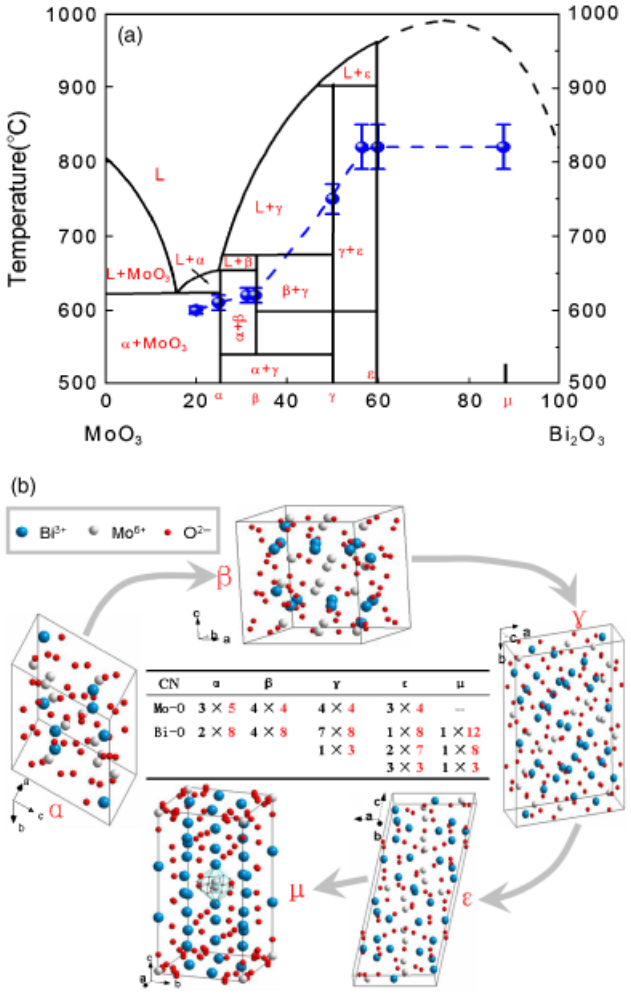

Fig. 1. Phase diagram (data from Kohlmuller and Badaud,[26] Egashira *et al.*,[27] Chen and Smith,[28] and Bleijenberg *et al.*[35]) and densification temperatures (solid dot with dash line) (a), typical crystal structures and coordination numbers in Bi_2O_3–MoO_3 system (b).

β and γ phases. The presence of four strongly bonded oxygens (with Mo–O distances below 0.20 nm) for each molybdenum site is a common feature to all bismuth molybdate phases with the exception of μ-$7Bi_2O_3$–MoO_3. All the bismuth molybdates in-

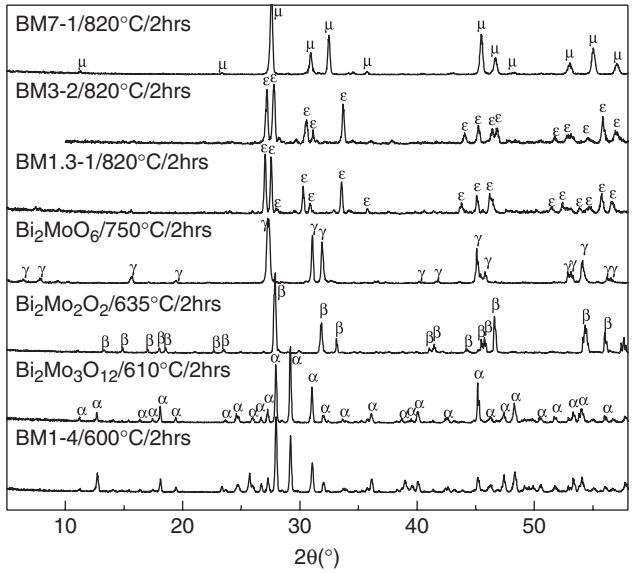

Fig. 2. X-ray diffraction patterns of Bi_2O_3–MoO_3 compounds sintered at different temperatures (α-$Bi_2Mo_3O_{12}$, β-$Bi_2Mo_2O_9$, γ-Bi_2MoO_6, ε-$Bi_{26}Mo_{10}O_{69}$ solid solution, and μ-$7Bi_2O_3$–MoO_3).

Table I. Microwave Dielectric Properties of Bi_2O_3–MoO_3 Compounds: α-$Bi_2Mo_3O_{12}$, β-$Bi_2Mo_2O_9$, γ-Bi_2MoO_6, ε-$Bi_{26}Mo_{10}O_{69}$, and μ-7Bi_2O_3–MoO_3

Compounds	Phase	ST (°C)	Frequency (GHz)	Permittivity	Q_f(GHz)	TCF (ppm/°C)
Bi_2O_3–4MoO_3	α+MoO_3	600±5	8.371	17±1.0	9300±400	−160±7.0
$Bi_2Mo_3O_{12}$	α	610±10	7.577	19±1.2	21 800±800	−215±9.0
Bi_2O_3–2.2MoO_3	α+β	620±10	5.739	35±1.5	12 000±500	−13±2.0
$Bi_2Mo_2O_9$	β	620±20	6.302	38±1.5	12 500±500	+31±3.0
Bi_2MoO_6	γ	750±20	6.434	31±1.2	16 700±500	−114±5.0
1.3Bi_2O_3–MoO_3	ε	820±30	8.057	26±1.2	4000±400	−139±5.0
3Bi_2O_3–2MoO_3	ε	820±30	6.193	31±1.2	1000±300	−41±4.0
7Bi_2O_3–MoO_3	μ	820±30	6.236	30±1.2	1900±300	+20±2.5

ST, sintering temperature; TCF, temperature coefficient of resonant frequency.

troduced in this work show a tendency for the bismuth sites to group into channels, which extend through the crystal structure. The molybdenum polyhedral forms a discontinuous framework around these channels. The coordination environment and bonding of the molybdenum cation might have the dominant role on the melting temperatures and the densification temperatures of Bi_2O_3–MoO_3 compounds. The densification temperatures are approximately 80%–90% of the melting temperatures of the compounds. As shown in Fig. 1(a), the sintering temperatures linearly increased from 600° to 750°C as x value increased from 0.2 to 0.5. When x value increased to 0.875, the sintering temperature of xBi_2O_3–$(1-x)MoO_3$ ceramic was maintained at around 820°C. In general, MoO_3-rich region possesses lower sintering temperatures than that of Bi_2O_3-rich region. More Bi atoms in structure will accelerate the discontinuity of molybdenum polyhedra. This could explain the increase of melting temperature and densification temperature when x value increases.

The phase compositions, sintering temperatures, and microwave dielectric properties of eight Bi_2O_3–MoO_3 compositions are summarized in Table I. Among all the compounds studied, the β-$Bi_2Mo_2O_9$ ceramic has the largest dielectric constant of 38 and a positive TCF value at about +31 ppm/°C. Near the $Bi_2Mo_2O_9$ composition, there are also two single phases, α-$Bi_2Mo_3O_{12}$ and γ-Bi_2MoO_6, and both have large negative TCF values of −215.0 and −113.8 ppm/°C, respectively. These three phases offered large design flexibility to obtain composite ceramics with adjustable TCF values by relative mixing of the phases, such as in the Bi_2O_3–2.2MoO_3 composition with both α and β phases providing a near-zero TCF about −13.4 ppm/°C. The high-frequency room-temperature permittivity is plotted as a function of Bi_2O_3 ratio across the Bi_2O_3–MoO_3 system. Also the TCFs are plotted as a function of permittivity and are shown in Figs. 3(a) and (b). The β-$Bi_2Mo_2O_9$ and Bi_2O_3–4MoO_3 compositions have the biggest and smallest permittivity, respectively. Dielectric constant in the microwave region is usually dominated by the ionic and electronic polarizability contributions of the oxide components. Attempts were made to calculate the respective permittivities of the Bi_2O_3–MoO_3 compounds using the oxide additivity rule,[38] but in all cases there were poor correlations and consistent underestimates in the magnitude of the permittivity, which suggest that small dipolar or order–disorder contributions may also exist in these compounds. TCFs are determined by both the linear thermal expansion coefficient α_l and the temperature coefficient of permittivity τ_ε.[39] Because α_l of microwave dielectrics is typically small (in the range of 0∼20 ppm/°C), TCF mainly depends on τ_ε. Although TCF values of all the microwave dielectric ceramics collected by Sebastian *et al.*[2] seemed to scatter randomly, τ_ε values were often found to be sensitive to the value of permittivity in many high-permittivity systems with similar composition or similar crystal structure.[40,41] For the Bi_2O_3–MoO_3 system, TCF values were found to be approximately linear to the permittivity as shown in Fig. 3(b). Bond valence considerations provided a useful way of examining bonding between every atom in particular structures.[42,43] The bond valence of each atom can be obtained from the actual bond length and parameters provided by Brown and Altermatt.[44] Then the apparent valences of atoms at each site can be obtained by simply summing over all neighbors' bond valences. Results for every cation site the valence sums are plotted in Fig. 4(a) as a function of Bi_2O_3 ratio in Bi_2O_3–MoO_3. It can be seen that for most phases both Bi and Mo have large valence deviations except for the β-$Bi_2Mo_2O_9$ and μ-7Bi_2O_3–MoO_3 phases. Valence deviation suggests the compressing or expanding of ions, which also means an unstable status of a cation at its position. The temperature coefficients as a function of the relative valence deviation of both Bi and Mo are also shown in Fig. 4(b). It is clear that larger valence deviation causes a larger TCF value. It can be inferred that ions with larger valences deviation will be more sensitive to temperature change than that with more normal valences. An exception was found for Mo valence deviation in α-$Bi_2Mo_3O_{12}$ phase. This may be caused by the different environment of Mo atom in

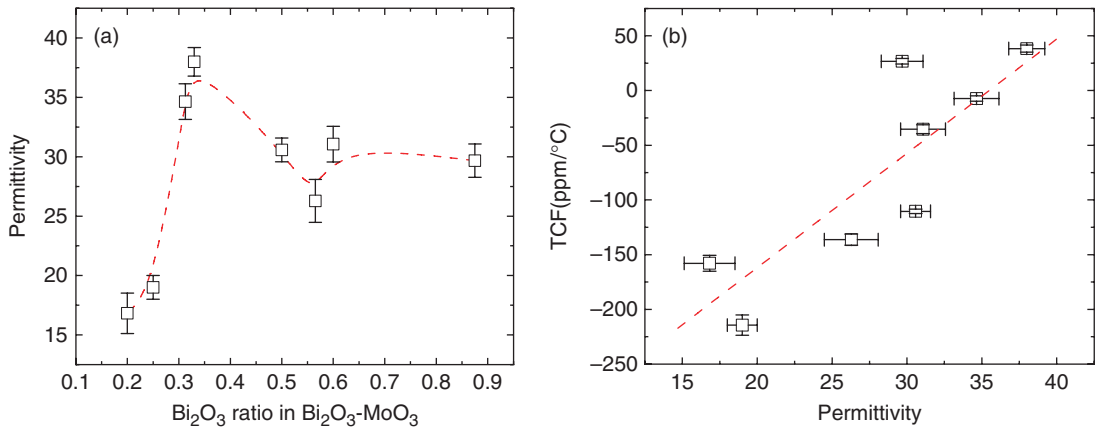

Fig. 3. Permittivity as a function of Bi_2O_3 ratio in Bi_2O_3–MoO_3 system (a) and temperature coefficient of resonant frequency as a function of permittivity (b).

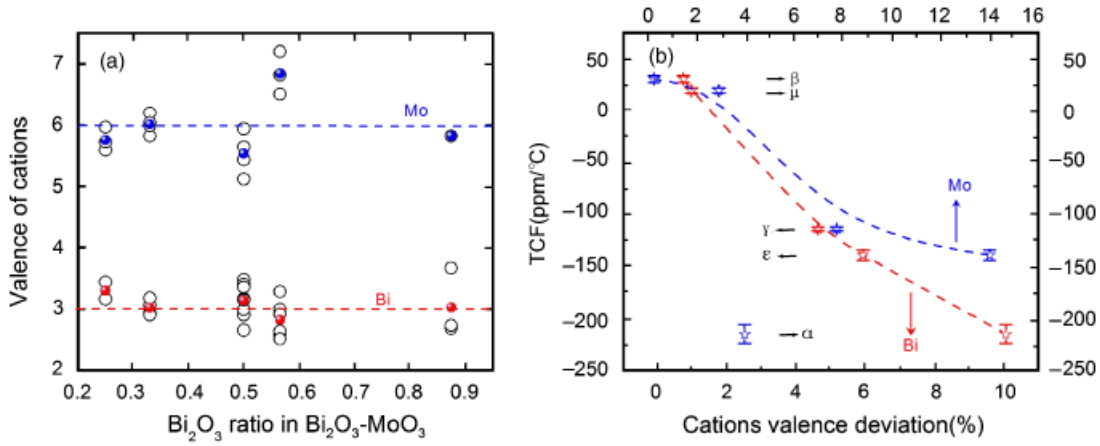

Fig. 4. Valence of each cation as a function of Bi_2O_3 ratio in Bi_2O_3–MoO_3 system (a) (hollow circle ○ for each atom and solid dot ● for mean values) and temperature coefficients of resonant frequencies as a function of the valence deviation of cations (b).

α-$Bi_2Mo_3O_{12}$ phase from other phases, i.e. a pentahedron rather than a tetrahedron. In fact, Bi^{3+} has nearly twice bigger polarizability than that of Mo^{6+} from the data reported by Shannon[45] and Choi *et al.*[46] Hence, the Bi valence deviation should dominate the change trend of TCF values.

Finally, a brief and preliminary investigation of the chemical compatibility of Bi_2O_3–MoO_3 compounds with common metal electrode materials is made. This was assessed by mixing 20 wt% Ag and 20 wt% Al powders with β-$Bi_2Mo_2O_9$, α-$Bi_2Mo_3O_{12}$, and Bi_2O_3–$4MoO_3$ samples, which were cofired at 600°~630°C for 4 h. The XRD patterns of Bi_2O_3–MoO_3 compounds cofired with 20 wt% Ag are shown in Fig. 5(a). In the MoO_3-rich region, Ag seemed more easy to react with MoO_3 and Bi_2O_3, and then formed new product phases of $AgBi(MoO_4)_2$ and other unidentified phases containing Ag and Mo. Figure 5(b) shows the XRD results of cofired samples with 20 wt% Al. For the β-$Bi_2Mo_2O_9$ and α-$Bi_2Mo_3O_{12}$ samples, only pure β-$Bi_2Mo_2O_9$, α-$Bi_2Mo_3O_{12}$, and aluminum phases were identified inferring that there were no chemical interactions. For the Bi_2O_3–$4MoO_3$ samples, an $Al_2(MoO_4)_3$ phase was formed with excess MoO_3. Although Mo is an active element that easily reacts with Ag and Al, the formation of bismuth-based compounds effectively suppress chemical reactions at these low temperatures. In summary, compounds in the Bi_2O_3–MoO_3 binary system are attractive candidate materials for an Ultra LTCC technology given the intrinsic low firing temperatures, excellent microwave dielectric

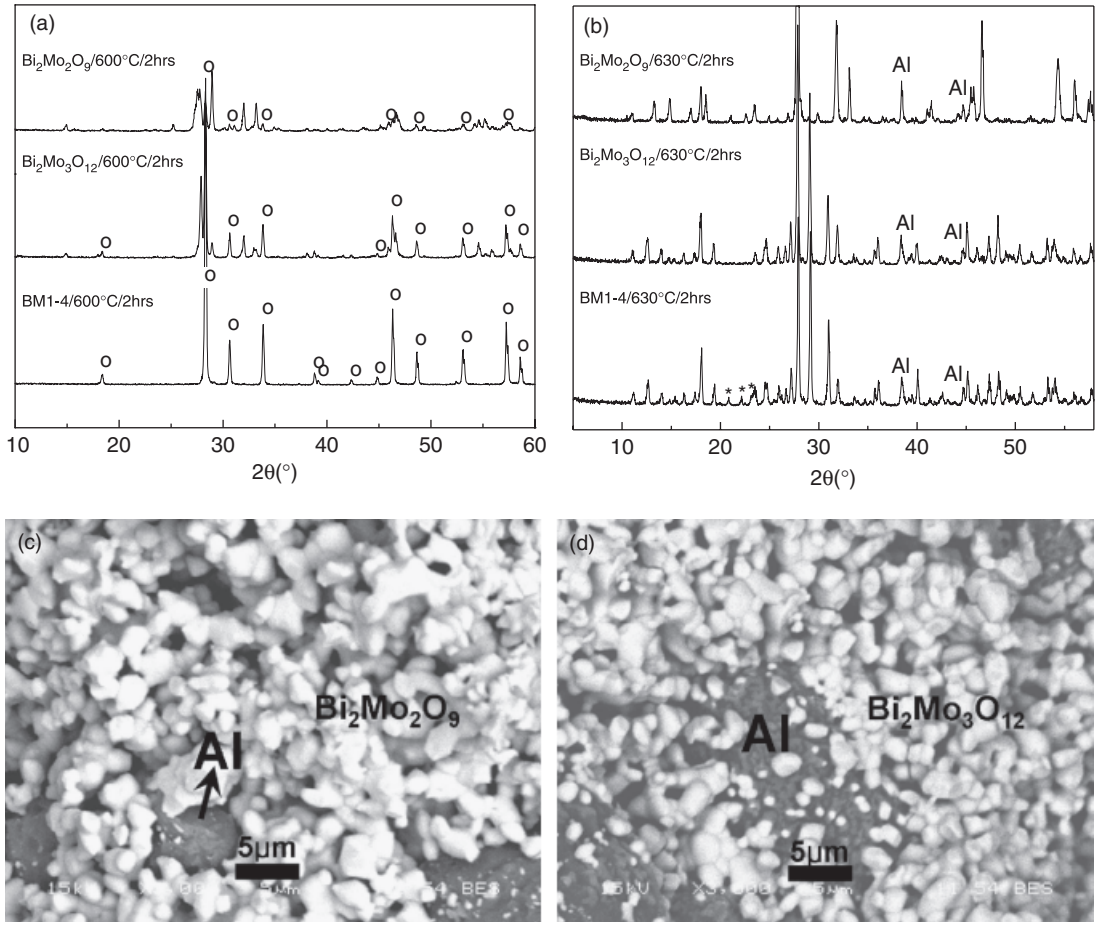

Fig. 5. X-ray diffraction patterns of Bi_2O_3–MoO_3 compounds cofired with 20 wt% Ag (a) and 20 wt% Al (b) at around 630°C (○, $AgBi(MoO_4)_2$; *$Al_2(MoO_4)_3$ (PDF:23-0764)), BEI photos of $Bi_2Mo_2O_9$ cofired with Al (c) and $Bi_2Mo_3O_{12}$ cofired with Al (d).

properties, and relatively high chemical stability with the electrode materials Al, at the low cofiring temperatures.

IV. Conclusions

A series of single phases and complex phases in Bi_2O_3–MoO_3 binary system that exhibited very low sintering temperature and good microwave dielectric properties was introduced. Among them the β-$Bi_2Mo_2O_9$ single phase has a dielectric constant of about 38, a Q_f of about 12 500 GHz, and a positive TCF of about +31 ppm/°C. Two other single phases near β-$Bi_2Mo_2O_9$ in the Bi_2O_3–MoO_3 binary diagram were α-$Bi_2Mo_3O_{12}$ and γ-Bi_2MoO_6 and they both have negative TCF values. This offered the possibility to design some complex phases with near-zero TCF values and Bi_2O_3–$2.2MoO_3$ designed in this work made an example. To apply this system in Ultra LTCC technology, we also studied the chemical compatibility of Bi_2O_3–MoO_3 system with silver and aluminum. It is found that Ag reacts with samples easily and forms a $AgBi(MoO_4)_2$ phase, whereas the β-$Bi_2Mo_2O_9$ and α-$Bi_2Mo_3O_{12}$ ceramics did not appear to react with aluminum at 630°C.

References

[1]R. R. Tummala, "Ceramic and Glass–Ceramic Packaging in the 1990's," *J. Am. Ceram. Soc.*, **74** [5] 895–908 (1991).

[2]M. T. Sebastian and H. Jantunen, "Low Loss Dielectric Materials for LTCC Applications: A Review," *Int. Mater. Rev.*, **53** [2] 57–90 (2008).

[3]O. A. Shlyakhtin and Y. J. Oh, "Low Temperature Sintering of $Zn_3Nb_2O_8$ Ceramics from Fine Powders," *J. Am. Ceram. Soc.*, **89** [11] 3366–72 (2006).

[4]C. L. Huang, R. J. Lin, and J. H. Wang, "Effect of B_2O_3 Additives on Sintering and Microwave Dielectric Behaviors of CuO-Doped $ZnNb_2O_6$ Ceramics," *Jpn. J. Appl. Phys., Part 1*, **41**, 758–62 (2002).

[5]N. Wang, M. Y. Zhao, and Z. W. Yin, "Effects of Ta_2O_5 on Microwave Dielectric Properties of $BiNbO_4$ Ceramics," *Mater. Sci. Eng. B*, **99**, 238–42 (2003).

[6]C. L. Huang and M. H. Weng, "The Microwave Dielectric Properties and the Microstructures of Bi(Nb, Ta)O_4 Ceramics," *Jpn. J. Appl. Phys., Part 1*, **38** [10] 5949–52 (1999).

[7]D. Zhou, H. Wang, X. Yao, and L. X. Pang, "Dielectric Behavior and Co-Firing with Silver of Monoclinic $BiSbO_4$ Ceramic," *J. Am. Ceram. Soc.*, **91** [4] 1380–3 (2008).

[8]I. S. Cho, J. R. Kim, D. W. Kim, D. W. Kim, and K. S. Hong, "Microwave Dielectric Properties and Far-Infrared Spectroscopic Analysis of $Ba_{5+n}Ti_nNb_4O_{15+3n}$ ($0.3<n<1.2$) Ceramics," *J. Eur. Ceram. Soc.*, **27**, 3081–6 (2007).

[9]R. Ratheesh, H. Sreemoolanadhan, S. Suma, M. T. Sebastian, K. A. Jose, and P. Mohanan, "New High Permittivity and Low Loss Ceramics in the BaO–TiO_2–Nb_2O_5 Composition," *J. Mater. Sci. Mater. Electron.*, **9**, 291–4 (1998).

[10]Q. Zeng, W. Li, J. L. Shi, J. K. Guo, M. W. Zuo, and W. J. Wu, "A New Microwave Dielectric Ceramic for LTCC Applications," *J. Am. Ceram. Soc.*, **89** [5] 1733–5 (2006).

[11]A. Y. Borisevich and P. K. Davies, "Crystalline Structure and Dielectric Properties of $Li_{1+x-y}Nb_{1-x-3y}Ti_{x+4y}O_3$ M-Phase Solid Solutions," *J. Am. Ceram. Soc.*, **85** [3] 573–8 (2002).

[12]S. X. Zhang, J. B. Li, J. Cao, H. Z. Zhai, and B. Zhang, "Effect of Composition on Sinterability, Microstructure and Microwave Dielectric Properties of $Zr_xTi_{1-x}O_4$ ($x = 0.40$–0.60) Ceramics," *J. Mater. Sci. Lett.*, **20**, 1409–11 (2001).

[13]C. L. Huang, C. S. Hsu, and R. J. Lin, "Improved High-Q Microwave Dielectric Resonator Using ZnO and WO_3-Doped $Zr_{0.8}Sn_{0.2}TiO_4$ Ceramics," *Mater. Res. Bull.*, **36**, 1985–93 (2001).

[14]H. J. Kim, S. Kucheiko, S. J. Yoon, and H. J. Jung, "Microwave Dielectrics in the $(La_{1/2}Na_{1/2})TiO_3$–$Ca(Fe_{1/2}Nb_{1/2})O_3$ System," *J. Am. Ceram. Soc.*, **80** [5] 1316–8 (1997).

[15]X. M. Chen, D. Liu, R. Z. Hou, X. Hu, and X. Q. Liu, "Microstructures and Microwave Dielectric Characteristics of $Ca(Zn_{1/3}Nb_{2/3})O_3$ Complex Perovskite Ceramics," *J. Am. Ceram. Soc.*, **87** [12] 2208–12 (2004).

[16]M. S. Fu, X. Q. Liu, X. M. Chen, and Y. W. Zeng, "Microstructure and Microwave Dielectric Properties of $(1-x)Ca(Mg_{1/3}Ta_{2/3})O_3/xCaTiO_3$ Ceramics," *J. Am. Ceram. Soc.*, **91** [4] 1163–8 (2008).

[17]M. Udovic, M. Valant, and D. Suvorov, "Phase Formation and Dielectric Characterization of the Bi_2O_3–TeO_2 System Prepared in an Oxygen Atmosphere," *J. Am. Ceram. Soc.*, **87**, 591–7 (2004).

[18]M. Udovic, M. Valant, and D. Suvorov, "Dielectric Characterisation of Ceramics from the TiO_2–TeO_2 System," *J. Eur. Ceram. Soc.*, **21**, 1735–8 (2001).

[19]M. Valant and D. Suvorov, "Glass-Free Low-Temperature Co-Fired Ceramics: Calcium Germanates, Silicates and Tellurates," *J. Eur. Ceram. Soc.*, **24**, 1715–9 (2004).

[20]D. K. Kwon, M. T. Lanagan, and T. R. Shrout, "Microwave Dielectric Properties of BaO–TeO_2 Binary Compounds," *Mater. Lett.*, **61**, 1827–31 (2007).

[21]D. K. Kwon, M. T. Lanagan, and T. R. Shrout, "Synthesis of $BaTiTe_3O_9$ Ceramics for LTCC Application and Its Dielectric Properties," *J. Ceram. Soc. Jpn.*, **113** [3] 216–9 (2005).

[22]D. K. Kwon, M. T. Lanagan, and T. R. Shrout, "Microwave Dielectric Properties and Low-Temperature Cofiring of $BaTe_4O_9$ with Aluminum Metal Electrode," *J. Am. Ceram. Soc.*, **88**, 3419–22 (2005).

[23]A. Feteira and D. C. Sinclair, "Microwave Dielectric Properties of Low Firing Temperature $Bi_2W_2O_9$ Ceramics," *J. Am. Ceram. Soc.*, **91** [4] 1338–41 (2008).

[24]G. Subodh and M. T. Sebastian, "Glass-Free $Zn_2Te_3O_8$ Microwave Ceramic for LTCC," *J. Am. Ceram. Soc.*, **90** [7] 2266–8 (2007).

[25]D. Zhou, H. Wang, X. Yao, and L.-X. Pang, "Microwave Dielectric Properties of Low Temperature Firing $Bi_2Mo_2O_9$ Ceramic," *J. Am. Ceram. Soc.*, **91** [10] 3419–22 (2008).

[26]R. Kohlmuller and J. P. Badaud, "Studies on System Bi_2O_3–MoO_3," *Bull. Soc. Chim. Fr.*, **10**, 3434–9 (1969).

[27]M. Egashira, K. Matsuo, S. Kagawa, and T. Seiyama, "Phase Diagram of the System Bi_2O_3–MoO_3," *J. Catal.*, **58**, 409–18 (1979).

[28]T. Chen and G. S. Smith, "The Compounds and the Phase Diagram of MoO_3-Rich Bi_2O_3–MoO_3 System," *J. Solid State Chem.*, **13**, 288–97 (1975).

[29]D. J. Buttrey, T. Vogt, U. Wildgruber, and W. R. Robinson, "Structural Refinement of the High Temperature Form of Bi_2MoO_6," *J. Solid State Chem.*, **111**, 118–27 (1994).

[30]D. J. Buttrey, T. Vogt, and B. D. White, "High-Temperature Incommensurate-to-Commensurate Phase Transition in the Bi_2MoO_6 Catalyst," *J. Solid State Chem.*, **155**, 206–15 (2000).

[31]R. N. Vannier, G. Mairesse, F. Abraham, and G. Nowogrocki, "$Bi_{26}Mo_{10}O_\delta$ Solid Solution Type in the Bi_2O_3–MoO_3–V_2O_5 Ternary Diagram," *J. Solid State Chem.*, **122**, 394–406 (1996).

[32]D. J. Buttrey, T. Vogt, G. Yap, and A. L. Rheingold, "The Structure of $Bi_{26}Mo_{10}O_{69}$," *Mater. Res. Bull.*, **32**, 947–62 (1997).

[33]D. J. Buttrey, "Compositional and Structural Trends Among the Bismuth Molybdates," *Top. Catal.*, **15**, 235–9 (2001).

[34]I. N. Belyaev and N. P. Smolynaninov, "Ternary System Bi_2O_3–MoO_3–PbO," *Zhur. Neorgan. Khimii*, **7**, 1126–31 (1962).

[35]A. C. A. M. Bleijenberg, B. C. Lippens, and G. C. A. Shuit, "Catalytic Oxidation of 1-Butene over Bismuth Molybdate Catalysts: I. The System Bi_2O_3–MoO_3," *J. Catal.*, **4** [5] 581–5 (1965).

[36]L. Y. Erman, E. L. Calpérin, and B. P. Soboler, "Phase Diagram of the Bismuth Sesquioxide–Molybdenum Trioxide System," *Zhur. Neorgan. Khimii*, **16** [2] 490–5 (1971).

[37]A. F. Van Den Elzen and G. D. Rieck, "The Crystal Structure of $Bi_2(MoO_4)_3$," *Acta Crystallogr. Sec. B: Struct. Crystallogr. Cryst. Chem.*, **29**, 2433–6 (1973).

[38]A. Heydweiller, "Dichte, Dielektrizitätskonstante und Refraktion fester Salze," *Z. Phys.*, **3**, 308–17 (1920).

[39]A. J. Bosman and E. E. Havinga, "Temperature Dependence of Dielectric Constants of Cubic Ionic Compounds," *Phys. Rev.*, **129**, 1593–600 (1963).

[40]P. J. Harrop, "Temperature Coefficients of Capacitance of Solids," *J. Mater. Sci.*, **4**, 370–4 (1969).

[41]D. Zhou, H. Wang, X. Yao, and L.-X. Pang, "Sintering Behavior and Microwave Dielectric Properties of $Bi_3(Nb_{1-x}Ta_x)O_7$ Solid Solutions," *Mater. Chem. Phys.*, **110**, 212–5 (2008).

[42]M. O'Keefe and N. E. Brese, "Atom Sizes and Bond Lengths in Molecules and Crystals," *J. Am. Chem. Soc.*, **113**, 3226–9 (1991).

[43]N. E. Brese and M. O'Keefe, "Bond-Valence Parameters for Solids," *Acta Cryst.*, **B47**, 192–7 (1991).

[44]I. D. Brown and D. Altermatt, "Bond-Valence Parameters Obtained from a Systematic Analysis of the Inorganic Crystal Structure Database," *Acta Crystallogr.*, **B41**, 244–7 (1985).

[45]R. D. Shannon, "Dielectric Polarizabilities of Ions in Oxides and Fluorides," *J. Appl. Phys.*, **73**, 348–66 (1993).

[46]G. K. Choi, J. R. Kim, S. H. Yoon, and K. S. Hong, "Microwave Dielectric Properties of Scheelite (A = Ca, Sr, Ba) and Wolframite (A = Mg, Zn, Mn) $AMoO_4$ Compounds," *J. Eur. Ceram. Soc.*, **27**, 3063–7 (2007). □